Supporting Information

Ruiz et al. 10.1073/pnas.1104009108

SI Materials and Methods

Clinical Samples. Pancreatic adenocarcinoma (PA) samples were obtained under a Western Institutional Review Board (WIRB) protocol (20040832) for a National Institutes of Health-funded biospecimens repository (National Cancer Institute P01 Grant CA109552). Participating centers included the Virginia Piper Cancer Institute (Minneapolis), Rush University (Chicago), University of Pittsburgh, Scottsdale Healthcare, and Banner Good Samaritan Medical Center (Phoenix). In addition, we obtained PA samples from the Eppley Institute, University of Nebraska Medical Center (Omaha, NE) Rapid Autopsy Program, funded in part by a Specialized Program in Research Excellence Grant (National Institutes of Health/National Cancer Institute 1P50CA127297) and Early Detection Research Network Biomarker Discovery Laboratory Grant (National Institutes of Health/National Cancer Institute 2U01CA111294).

Scanning and Data Processing. All microarray slides were scanned using an Agilent 2565C DNA scanner, and the images were analyzed with Agilent Feature Extraction version 10.5 using default settings. The array comparative genomic hybridization (aCGH) data were assessed with a series of quality control metrics and then analyzed using an aberration detection algorithm (ADM2) (1). The latter identifies all aberrant intervals in a given sample with consistently high or low log ratios based on the statistical score derived from the average normalized log ratios of all probes in the genomic interval multiplied by the square root of the number of these probes. This score represents the deviation of the average of the normalized log ratios from its expected value of zero and is proportional to the height, h (absolute average log ratio), of the genomic interval and to the square root of the number of probes in the interval.

Microarray File Deposition. All microarray files have been deposited at the National Center for Biotechnology Information Gene Expression Omnibus (accession no. GSE21660).

Sequencing. We used the RainDance Technologies emulsion PCR system to PCR-amplify the RDT 1000 oligo set, which represents a validated set of ∼4,000 exons for mutational analysis of thre distinct flow-sorted populations isolated from a patient treated with androgen ablation therapy who developed metastatic prostate adenocarcinoma (PC). We used the Applied Biosystems/Life Technologies SOLiD system, version 3.0 fragment library methodology for these analyses. In addition, the eight exons of the *AR* gene were sequenced using conventional technologies. All assays were done through the TGen Sequencing Facility.

Fluorescence in Situ Hybridization. For quantification of centromeres, Vysis CEP3 (Spectrum Red) and Vysis CEP7 (Spectrum Green) (Vysis, Abbott Laboratories) were used. For *AR* gene copy analysis, the LSI Androgen Receptor probe (Vysis) and the Vysis CEPX (Spectrum Green) were used. *ETV6* break was analyzed by using the LSI ETV6 (TEL) probe (Vysis). Before hybridization, slides were treated according to the Paraffin Pretreatment Reagent Kit protocol (Vysis). Hybridization and post-hybridization washes were according to the Vysis LSI procedure. Images were obtained by using a Zeiss Axioplan 2 fluorescence microscope (Zeiss) equipped with an ISIS-digital camera (MetaSystems). All images were acquired with a 100× objective (Plan-Apochromat, Zeiss).

PCR. PCR analysis of *FOXO3A* and neighboring genes (*LACE1* and *ARMC2*) was performed by using the AmpliTaq Gold DNA Polymerase (Applied Biosystems) according to the manufacturer's instructions. Briefly, flow-sorted and phi29-amplified DNA was subjected to a PCR composed of 35 cycles with an annealing temperature of 58 °C. The following primers were used: *LACE1*—forward (5-GGCCTGAGGGATGGGTCGCT-3) and reverse (5-GGCTGGCTCCTGGCTGGTTC-3); *FOXO3A* first set—forward (5-GGTCTGGCCACCTCAATCCAGACT-3) and reverse (5-AAACCTCCTCCCAAACGCCAGAGT-3); *FOXO3A* second set—forward (5-TGCAAGTTGCTGGCCAGGTT-3) and reverse (5-ACGGCACTGCCTTCCTGTGG-3); *ARMC2*—forward (5-TTGGGGATGGGCGATCCAGGG-3) and reverse (5-ACGCGGCAGTTCTGTGTGCAT-3). PCR products and the DNA molecular weight marker VIII (Roche Applied Bioscience) were separated on a 1% agarose gel and visualized using the Alphaimager System (Cell Biosciences).

1. Lipson D, Aumann Y, Ben-Dor A, Linial N, Yakhini Z (2006) Efficient calculation of interval scores for DNA copy number data analysis. *J Comput Biol* 13:215–228.

Cycle	%G1	%G2	%S	%Total	D.I.
Diploid	100.00	0.00	0.00	50.02	n/a
Aneuploid A	81.21	8.09	10.70	49.98	1.90

Cycle	%G1	%G2	%S	%Total	D.I.
Diploid	88.76	0.00	11.24	27.94	n/a
Aneuploid	76.85	16.47	6.67	72.06	1.18

Fig. S1. Flow sorting (*A*) and whole-genome aCGH profiles (*B*) of 3.8N PC clonal population with >100 ADM2-defined intrachromosomal intervals. (*C–E*) Detection of homozygous deletions in PA. (*C*) A 2.3N population representing >70% of total cell content was sorted from a PA sample. The homozygous deletion in *SMAD3* on chromosome 15q23 was detected in the (*D*) sorted sample but missed in the (*E*) bulk sample. Blue-shaded areas represent aberrations as called by ADM2.

Fig. S2. (*A*) CGH analyses of an unsorted PC sample. *AR* (Xq12) amplification was detected in both sorted and unsorted (bulk) samples. However, the height of the amplicon is compressed in the nonsorted sample. (*B–D*) Analysis of PA biopsy P1026Z. (*B*) DAPI-based DNA content analysis detected a 3.7N population representing 7.6% of the cellular content of the biopsy. (*C*) Only the 3.7N population showed homozygous deletions and focal amplicons. (*D*) Close-up view of the *VEGFA* amplicon and the *JARID2A* deletion.

Fig. S3. Concurrent aberrations in a PA genome. (*A*) A 3.0N aneuploid population representing only 3% the cellular content of the PA biopsy sample was profiled with 244,000 feature aCGH. (*B*) Genome view of the 3N aneuploid population. (*C*) Gene and chromosome view of the 19p13 amplification. (*D*) Gene and chromosome view of the 18p11 amplification.

Fig. S4. Analysis of a PA biopsy. (*A*) DAPI-based DNA content analysis detected two aneuploid populations (2.3 and 3.8N). (*B–F*) Overlay of the 2.3N (red) and the 3.8N (blue) CGH profiles. (*B*) Genome view of both aneuploid genomes. (*C*) View of the CGH profile of chromosome 8 including two separate breakpoints (arrows). (*D*) View of the CGH profile of chromosome 19 including the 19q13.2 amplicon. (*E*) Locus-specific view of the breakpoint at 8q13.2. (*F*) Locus-specific view of the 8q23.3 breakpoint.

Fig. S5. Clonal analysis of a PC metastasis originally diagnosed as adrenal cortical carcinoma. (*A*) Detection of *AIM1* (6q12) homozygous deletion. (*B*) Validation of the *TP53* homozygous deletion. Genomic DNA from normal reference and 3.8N clone were screened by PCR assays for *TP53* exon 1 (lanes a and d) *TP53* exon 8 (lanes b and e) and *FGFR2* exon 7 (lanes c and f). The PCR product for the *TP53* exon 8 includes the sequence of the single 60mer CGH probe that had the $\log_2$ ratio of −3.5. (*C*) Knowledge mining and predictive modeling of the patient-specific clonal context. The interactions of the selected clonal lesions are summarized. The loss of *PTEN* and activation of *AKT1* leads to stimulation of the AR gene followed by transcriptional stimulation of the *ERG*-dependent oncogenic transcriptional program via the *TMPRSS2:ERG* fusion gene (schematic was generated with MapEditor software from GeneGO). (*D*) The homozygous deletions (*PTEN*, *AIM1*, *TP53*) and the interstitial deletion (5′ boundary *ERG* gene) can be detected only in the sorted (blue line), not in the preparation from the bulk tissue (red line).

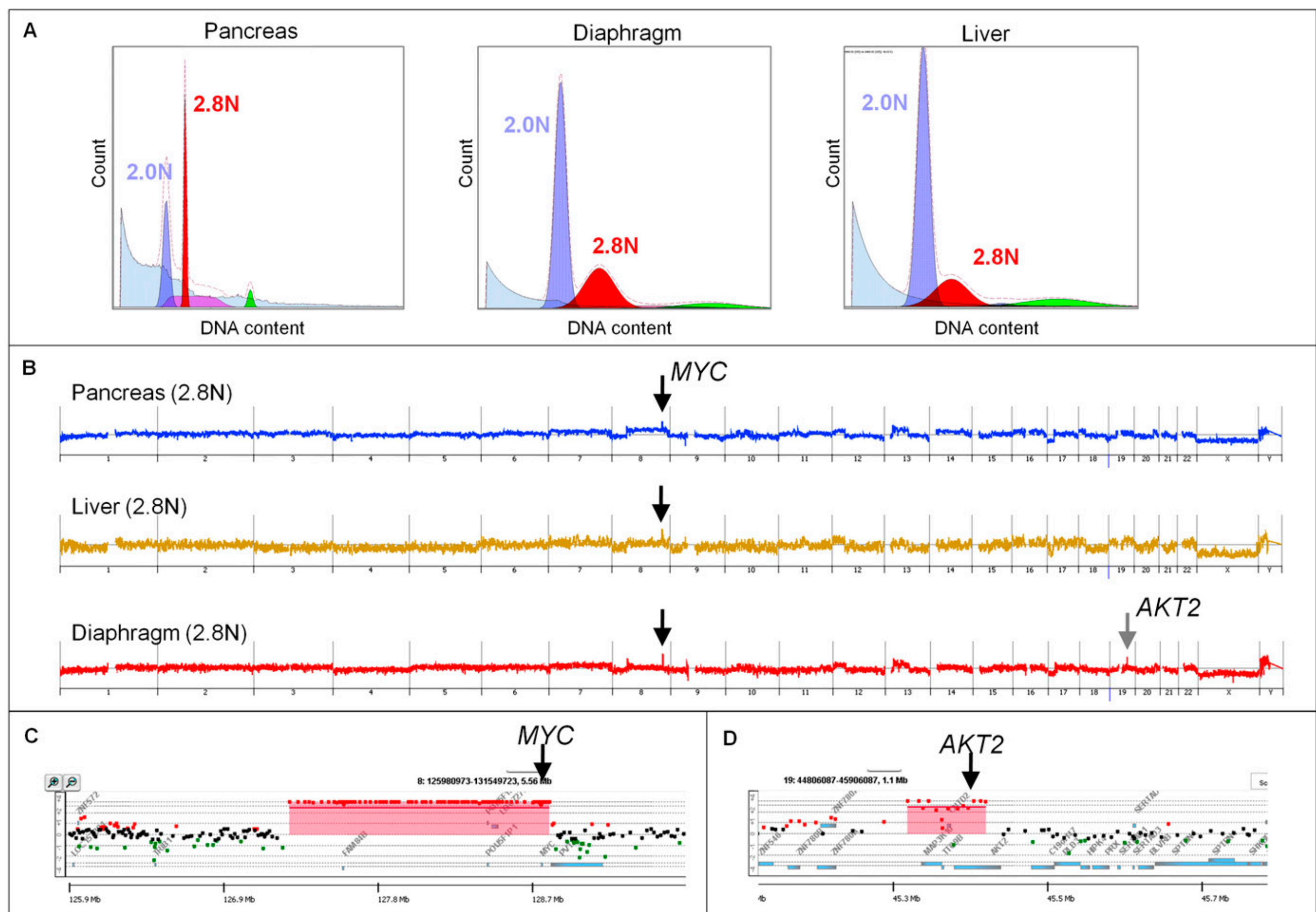

Fig. S6. Clonal analysis of a PA rapid autopsy. (*A*) DAPI-based DNA content analyses of a primary (pancreas) and two metastases (diaphragm and liver) detected a 2.8N clonal population in each anatomical site. (*B*) Genomes of the three 2.8N sorted populations. The *MYC* amplicon is present in all three populations. The *AKT2* amplicon is specific for the metastasis in the diaphragm. (*C*) Locus-specific view of the *MYC* amplicon in the aneuploid population of the diaphragm. (*D*) Locus-specific view of the *AKT2* amplicon in the aneuploid population of the diaphragm.

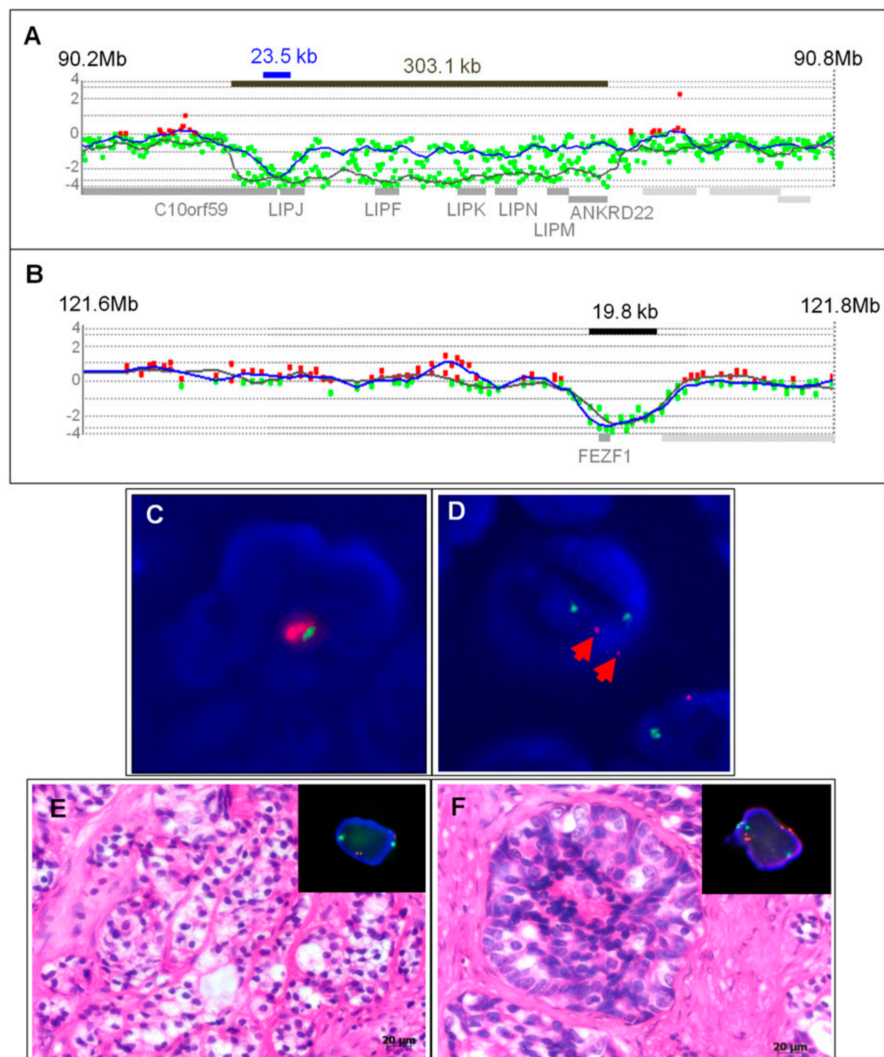

Fig. S7. Genomic profiling of distinct clonal populations within a castration-resistant PC. (*A*) The aneuploid population (brown line) harbors a wider homozygous deletion on 10q23 than the diploid tumor population (blue line). (*B*) Some homozygous deletions, such as the deletion of the *FEZF1* gene (7q31), are shared by both populations. (*C*) FISH validation of the *AR* gene amplification: the low-level amplification is also visible by FISH. (*D*) FISH analysis with a 9p21 commercially available FISH probe does not show the 9p21 deletion. (*E*) Histological and FISH analysis (*Inset*) of centromere 3 (red) and 12 (green) of the diploid population. (*F*) Histological and FISH analysis (small box) of centromere 3 and 12 of the aneuploid population. Red arrowheads point toward the 9p21 FISH signals. Horizontal light gray bars without gene names represent genes that do not show genomic aberrations.

Fig. S8. Clonal analysis of a PA rapid autopsy. (*A*) The 9p21 (*CDKN2A*) homozygous deletion is shared by all aneuploid populations, but not by the normal 4N (G_2/M) lung population. (*B*) The 19q13 amplicon is found only in the 6N population from the lung. (*C*) Exemplary locus-specific views of genomic aberrations: The homozygous deletions of *CDKNA2* and *NRG3* are not present in the genomically normal 4N (G_2/M) lung population. The 19q13 (*RHPN2*) and the 8p23 (*BLK*) are present only in the 6N lung population. Red line, lung (6N); brown line, lung [4N (G_2/M)]; blue line, pancreas (4.5N); PA, pancreas; LI, liver; DI, diaphragm; LU, lung; AN, aneuploid.

Fig. S9. Genomic profiling and FISH analysis of the populations of the multibiopsy series from a patient with PC. (*A*) The CGH profile of chromosome X of the aneuploid population from 2007 shows broad high-level amplification that includes the *AR* (black arrow). (*B* and *C*) The diploid populations from 2007 (*B*) and 2008 (*C*) harbor a small focal *AR* gene amplification (399 kb). (*D*) The copy-number transition between the *ELK4* and the *SLC45A3* gene is shared by all populations. (*E*) The copy-number transition upstream of the *ETV6* gene is shared by all populations. (*F*) Homozygous deletion of the *FOXO3A* gene is detected only in the 2N population from 2008. (*G*) PCR validation of the *FOXO3A* gene deletion in the population from 2008. (*H*) *AR* FISH analysis of the diploid population from 2000 shows normal *AR* gene copy status: *AR* gene (red), centromere X (green). (*I*) *AR* FISH analysis of the diploid population from 2007 confirms the focal *AR* gene amplification. (*J*) *AR* FISH analysis of the aneuploid population from 2007 shows the Xq12 amplicon including multiple copies of the *AR* gene and of the chromosome X centromere. (*K*) *AR* FISH analysis of the diploid population from 2008 confirms the focal *AR* gene amplification. (*L*) Validation of the copy-number transition upstream of the *ETV6* gene by FISH. The copy-number transition upstream of the *ETV6* gene was confirmed by using an *ETV6* FISH break-apart rearrangement probe: one single red signal with loss of one green signal.